RESEARCH ARTICLE | SEPTEMBER 19 2024

A non-autonomous framework for climate change and extreme weather events increase in a stochastic energy balance model ⊕

G. Del Sarto ; F. Flandoli ✉

Check for updates

View Online   Export Citation

A non-autonomous framework for climate change and extreme weather events increase in a stochastic energy balance model ⓔⓟ

View Online   Export Citation   CrossMark

G. Del Sarto[1,2,a] ⓘ and F. Flandoli[1,b] ⓘ

AFFILIATIONS

[1] Class of Science, Scuola Normale Superiore, 56126 Pisa, Italy
[2] Department of Science, Technology and Society, University School for Advanced Studies IUSS Pavia, 27100 Pavia, Italy

Note: This paper is part of the Focus Issue, Nonautonomous dynamics in the climate sciences.
[a] **Electronic mail:** gianmarco.delsarto@sns.it
[b] **Author to whom correspondence should be addressed:** franco.flandoli@sns.it

ABSTRACT

We develop a three-timescale framework for modeling climate change and introduce a space-heterogeneous one-dimensional energy balance model. This model, addressing temperature fluctuations from rising carbon dioxide levels and the super-greenhouse effect in tropical regions, fits within the setting of stochastic reaction–diffusion equations. Our results show how both mean and variance of temperature increase, without the system going through a bifurcation point. This study aims to advance the conceptual understanding of the extreme weather events frequency increase due to climate change.

In recent years, the increase in the frequency and intensity of extreme weather events has become one of the most dangerous consequences of climate change. Despite this, understanding the mechanisms that drive these phenomena remains uncertain. This paper presents a framework that differentiates between climate, weather, and an intermediate scale termed macroweather. In the first part, we justify the presence of noise, following Hasselmann's approach, in the equations representing the temperature at the macroweather scale. We also explain why a non-autonomous term with a slower timescale, such as carbon dioxide concentration, can be considered adiabatic (in thermodynamics, a gas undergoes an adiabatic transformation during rapid expansion or compression; although fast, the transformation is slow enough that the gas stays in the state of statistical equilibrium and the transformation preserves the entropy of the gas. Here, and throughout the text, we use the term "adiabatic" to refer to a variable that varies much more slowly than the timescale of the system of which it is a part), i.e., constant, at the macroweather scale. In the second part, we introduce a new one-dimensional energy balance model, an elementary model that fits within our abstract framework and assumes Earth's temperature evolves according to the radiation absorbed and emitted by the planet. The novelty of our model lies in incorporating a parametrization of the super-greenhouse effect, a feedback mechanism that can lead to instability in the tropics due to Earth's radiation. By adding additive noise to our model, we numerically investigate and explain the observed increase in temperature fluctuations in response to adiabatic changes in atmospheric CO_2 concentration.

I. INTRODUCTION

The purpose of this paper is twofold: to describe a scheme for a three-timescale non-autonomous dynamical system suitable for the description of climate change and to present a new example of an energy balance model (EBM) with spatial structure. This model fits into our abstract framework and may contribute to a conceptual explanation of the increased frequency of extreme events. The non-autonomous nature of this example is crucial, making its connection to the foundational scheme particularly interesting.

It is essential to emphasize two key aspects. First, the three-timescale scheme is designed to motivate the structure of the

20 September 2024 07:18:12
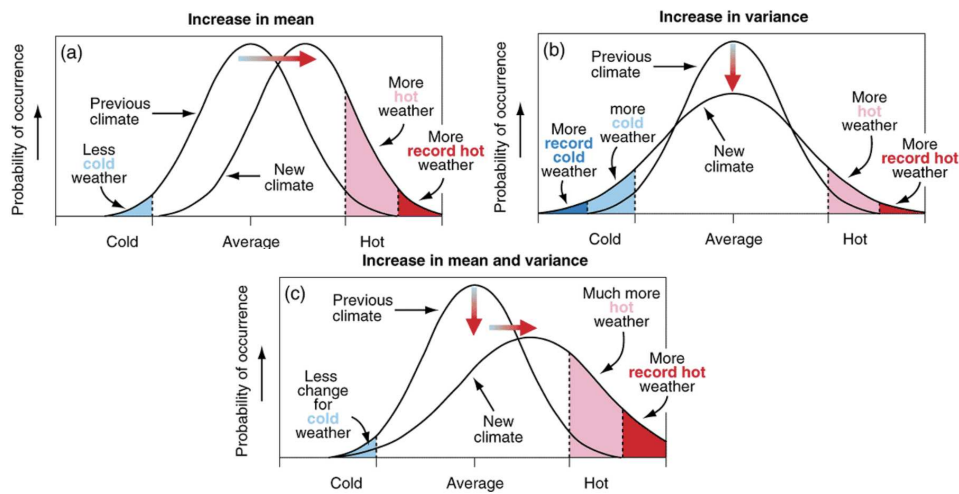
FIG. 1. Schematic showing the effect on extreme temperatures when (a) the mean temperature increases, (b) the variance increases, and (c) when both the mean and variance increase for a normal distribution of temperature. Reproduced from the IPCC Report on Climate Change 2001: The Scientific Basis, Ref. 1, Fig. 2.32.

proposed EBM, including the adiabatic CO_2 variable, the presence of noise, and the system's timescale. Second, the EBM in question is a simplified climate model, representing the lowest level of complexity among climate models. As such, it can only provide qualitative insights into climate dynamics. Therefore, we deliberately avoid making quantitative comparisons between our model's results and real-world data.

From the viewpoint of climate change analysis, our goal is to provide a simplified model that demonstrates how temperature fluctuations increase with rising carbon dioxide (CO_2) concentrations. Probably, the most dramatic example of climate change today is the increased frequency of extreme events. As pointed out by the IPCC Report, Ref. 1, this can result from both an increase in the mean temperature and an increase in the variance of temperature, as shown in Fig. 1, not only by the increase in the mean value but also by the increase in the variance of a climatic variable.

This phenomenon is not just speculative and can be observed by looking at real data, as can be done in Fig. 2(a). It shows the histogram of the daily mean temperature recorded in August in two different periods, from 1910 to 1940 in blue, and from 1993 to 2023 in red. In our opinion, being able to explain the joint increase in mean value and variance is a challenging and, at the moment, a completely open question. Indeed, a classical paradigm to explain the increase in the frequency of extreme events is given by a dynamical system approaching a bifurcation point, a system subject to random fluctuations, which are amplified near the bifurcation point.[2–8] But the main question then is whether the Earth, nowadays, is close to a bifurcation point or not, an issue which is speculated but not proven. Looking to the far past, it is rather clear that bifurcations took place connecting a moderate climate like our own today with glacial climates. But a clear indication that now we are close to a new bifurcation point in the direction of a warmer climate is missing. Except for certain data near the Tropics: localized in space at

that latitude, there is experimental evidence of a potential bistability and, therefore, of the possibility of a fast transition to a warmer climate.[9] But far from the Tropics, the data are different. Therefore, we have developed a space-dependent model that incorporates this difference. Seen globally, as an infinite dimensional dynamical system on the whole globe, the Tropics bistability does not add a new bifurcation to the model.

We focus on the class of EBMs, which give an elementary, yet useful, representation of Earth's climate by capturing the fundamental mechanisms governing its behavior.[7,10–15] This type of models, which describes temperature evolution, assumes that it evolves according to the radiation balance of the budget, i.e., the difference in the radiation absorbed and emitted by the planet. Other key factors, such as insolation, atmospheric composition, and surface properties, are considered in EBMs in order to get a radiation budget as accurate as possible.

More in detail, we work with a Budyko–Sellers one-dimensional energy balance model (1D EBM), in which a diffusion term modeling meridional heat transport is added as a driver of temperature evolution.[16] The novelty of our model consists in adding, for the first time, a particular phenomenon that may happen at the Tropics. Indeed, one of the key mechanisms to stabilize Earth's temperature is the Planck feedback. It consists of an increase in outgoing longwave radiation (OLR) as surface temperature increases, thanks to the Stefan–Boltzmann law. But there exist cases, and our model highlights one of them, where this feedback can fail, as in the super-greenhouse effect (SGE).[9,17,18] This phenomenon is feedback between water vapor, surface temperature, and greenhouse effect. Once the sea surface temperature or greenhouse gas concentration reaches a certain level, the increase in absorbed thermal radiation from the surface due to augmented evaporation with rising sea surface temperature (SST) outweighs the concurrent elevation in OLR, causing OLR to decline as SST increases.

(a)   (b)
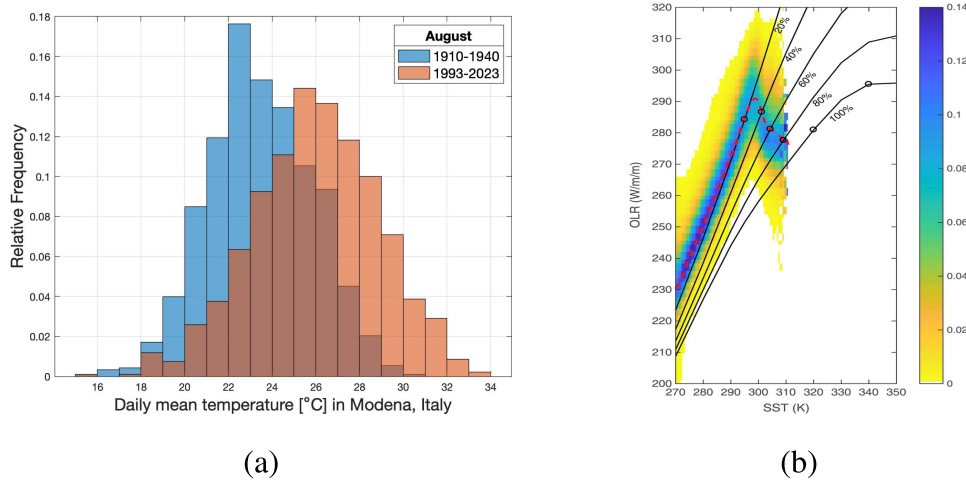
FIG. 2. (a) Daily temperature recorded in August in Modena, Italy. The blue histogram shows the values for the time period 1910–1940 (blue), and the red histogram refers to 1993–2023 (red). Data provided by the Osservatorio Geofisico di Modena, www.ossgeo.unimore.it. (b) Observational Outgoing Longwave Radiation (OLR) dependence on Sea Surface Temperature (SST), and SMART (SMART is a dataset for OLR measurements used in Ref. 9) OLR output for various humidity values. The red dashed line is the mean. Reproduced with permission from Dewey and Goldblatt, Geophys. Res. Lett. **45**, 10673–10681 (2018). Copyright 2018, John Wiley and Sons [Ref. 9, Fig. 2(a)].

From the mathematical viewpoint, the EBM proposed here is a non-autonomous stochastic partial differential equation (SPDE) of reaction–diffusion type.[19,20] The non-autonomy stands in a slowly varying term corresponding to CO_2 concentration. We clarify the link between such a scheme and a more classical adiabatic approach, where the slowly varying term is kept constant and the long-term behavior of the corresponding autonomous dynamical system is investigated. It is worth pointing out that the timescale of our model is intermediate between the daily timescale of weather and the centurial timescale of climate. It is sometimes called macroweather, and it is of the order of a month to one year. For this reason, the abstract framework of a two-timescale separation of a non-autonomous dynamical system is introduced to describe the macroweather-climate dichotomy, interpreting the weather as a faster timescale than macroweather which is averaged out by looking at the temperature on time interval of months.

This paper is organized as follows. In Sec. II, we introduce the non-autonomous framework for weather, macroweather, and climate, with a particular focus on the latter two. We outline the scale separation between them and provide their tentative definitions. This first, abstract part culminates in a link between macroweather and climate, justifying an adiabatic approach to studying the former in the presence of a non-autonomous dependence, such as CO_2 concentration in the atmosphere. In Sec. III, we begin by recalling the key concepts of EBMs, starting with the zero-dimensional version in Sec. III A. We discuss why EBMs are suitable for describing macroweather and how they can explain the increase in global mean temperature (GMT) due to rising CO_2 concentrations. In Sec. III B, we introduce our new 1D EBM, detailing the parametrization of all the terms of the parabolic partial differential equation (PDE). Section III C describes the deterministic properties of the model, such as the existence of one or more steady-state solutions and their

dependence on the CO_2 parameter. In Sec. III D, we discuss the stochastic extension of the model and its properties, including the existence of an explicit invariant measure. Section III E presents the main results of the second part. We demonstrate how our model predicts an increase in the variance of temperature fluctuations under CO_2 in the current climate configuration, without introducing new bifurcation points. We use both numerical tools and theoretical arguments to explain and understand this phenomenon. Finally, Sec. IV summarizes our findings, while Appendixes A and B detail the finite-difference scheme used for numerical simulations and some spectral properties needed to deduce the existence of the invariant measure for the stochastic problem.

II. THE NON-AUTONOMOUS SCHEME WITH THREE TIMESCALES

In Sec. III, we introduce a stochastic EBM with suitable space dependence, and a slowly varying parameter corresponding to CO_2 concentration, in order to investigate the time change of fluctuations, as also discussed in Sec. I. There are three different timescales involved in this modeling. We could skip the first one by just mentioning Ref. 21 and restrict ourselves to two timescales only, but at the same time we want to insist on the non-autonomous structure of the modeling, hence it is convenient to enlarge the discussion a bit.

In the modeling we have in mind, there are three timescales, called

- weather, where variations are visible at the timescale of hours/day [variables will be denoted by $V_w(t)$, $T_w(t)$ etc.];
- macroweather, where variations are visible at the timescale of months/year [variables will be denoted by $V_{mw}(t)$, $T_{mw}(t)$ etc.];

- climate, changing at the timescale of dozens of years (probability measures and their expected values characterize this level, still changing in time).

Subdivision and attribution of a precise timescale are not strict.

Remark 1 The reader will realize that, for the purpose of Sec. III, we could start from Subsection II E. Let us then explain why we think that Subsections II A–II D are also very important. As already said, the main purpose of this work is to identify possible explanations for an increase in variance, when a parameter changes. In a sentence, the two main ingredients are a noise in the system equations and a suitable nonlinearity which amplifies the variations of the noise in a different way for different values of the parameter. The noise, then, is crucial. Subsections II A–II D are devoted to explaining its origin.

A. The weather timescale

Following Ref. 21, it is natural to model the weather scale by deterministic equations, ordinary equations for simplicity of notation (but the ideas are the same for PDEs); randomness can be introduced but it is not strictly necessary, except maybe for a description of the uncertainty about initial conditions and parameters, not included in the present discussion. Following Ref. 21, we distinguish the main physical variables into fast and slow ones, according to a system of the form

$$\partial_t V_w = f(V_w, T_w),$$
$$\partial_t T_w = \epsilon g\left(V_w, T_w, q(\epsilon t)\right),$$
$$q(t) \text{ slowly varying,}$$

for a small $\epsilon > 0$. Here, V_w changes in unitary time (corresponding to hours/day), and T_w varies very slowly (monthly, say). In addition, the slow variable is influenced by a slow time change of structure, described by the time-varying parameters $q(\epsilon t)$. The function $q(t)$ is assumed to be slowly varying, hence $q(\epsilon t)$ *is super-slowly varying* (from here the three timescales arise).

The parameter $\tau = \frac{1}{\epsilon}$ corresponds to the typical reaction time of the slow variables, measured in the unitary time of V. Appreciable changes of T happen in a time of order τ, at the weather scale.

With great simplification, we may think that V collects the fluid dynamic variables (the fluid *V*elocity plus other related variables), which are very unstable and rapidly changing at the daily level, while T represents *T*emperature. In this case, the unit of time at the weather level is of the order of hours, and $\tau = \frac{1}{\epsilon}$ is of the order of a few months, hence, e.g., of order 100. On the contrary, the time change of CO_2 concentration, call it τ_{CO_2}, is of the order of a dozen of years, hence, e.g., of order 10 000 in the weather scale. With these figures, $q(t)$ has a relaxation time of 100 and $q(\epsilon t)$ of order 10 000.

B. Macroweather timescale for *T*

Then, we change the scale and set

$$\widetilde{T}_{mw}(t) = T_w\left(\frac{t}{\epsilon}\right),$$

so that we observe variations of $\widetilde{T}_{mw}(t)$ in unitary time. We call this the macroweather timescale. It holds

$$\partial_t \widetilde{T}_{mw}(t) = g\left(V_w\left(\frac{t}{\epsilon}\right), \widetilde{T}_{mw}(t), q(t)\right).$$

Let us recall that, at this timescale, q varies very slowly. Let us look for a simplification of this equation, where V_w does not appear any more.

C. The averaging approximation

Let us heuristically describe the averaging approximation, which can be made rigorous under proper assumptions for suitable systems, see Ref. 22.

At the integral level, we have

$$\widetilde{T}_{mw}(t) - \widetilde{T}_{mw}(t_0) = \int_{t_0}^t g\left(V_w\left(\frac{s}{\epsilon}\right), \widetilde{T}_{mw}(s), q(s)\right) ds.$$

If $t - t_0$ is small, let us use the reasonable approximation

$$\sim \int_{t_0}^t g\left(V_w\left(\frac{s}{\epsilon}\right), \widetilde{T}_{mw}(t_0), q(t_0)\right) ds$$

$$= (t - t_0)\frac{1}{t - t_0}\int_{t_0}^t g\left(V_w\left(\frac{s}{\epsilon}\right), \widetilde{T}_{mw}(t_0), q(t_0)\right) ds.$$

Then, if $\epsilon << t - t_0$, we heuristically invoke an ergodic theorem and approximate

$$\sim (t - t_0)\int g\left(v, \widetilde{T}_{mw}(t_0), q(t_0)\right) v_{\widetilde{T}_{mw}(t_0)}(dv),$$

where $v_\tau(dv)$ is invariant for

$$\partial_t V = f(V, \tau).$$

Setting

$$\bar{g}(\tau, q) = \int g(v, \tau, q) v_\tau(dv),$$

we may write

$$= (t - t_0)\bar{g}\left(\widetilde{T}_{mw}(t_0), q(t_0)\right),$$

and then again approximate it to

$$\sim \int_{t_0}^t \bar{g}\left(\widetilde{T}_{mw}(s), q(s)\right) ds.$$

Hence, we get the simplified model

$$\partial_t \overline{T}_{mw}(t) = \bar{g}\left(\overline{T}_{mw}(t), q(t)\right).$$

D. Hasselmann's proposal

However, in our case, this simplification is not realistic. If ϵ is of order $\frac{1}{100}$, then $t - t_0$ is of order one, because we need the validity

of the approximation

$$\frac{1}{t-t_0} \int_{t_0}^{t} g\left(V_w\left(\frac{s}{\epsilon}\right), a, b\right) ds \sim \int g\left(v, a, b\right) \nu_a\left(dv\right).$$

But on a time of order one, we observe variations of $\widetilde{T}_{mw}(t)$, we said above, hence the approximation,

$$\int_{t_0}^{t} g\left(V_w\left(\frac{s}{\epsilon}\right), \widetilde{T}_{mw}(s), q(s)\right) ds$$
$$\sim \int_{t_0}^{t} g\left(V_w\left(\frac{s}{\epsilon}\right), \widetilde{T}_{mw}(t_0), q(t_0)\right) ds,$$

is not so strict [on the contrary, it is excellent for the $q(s) \sim q(t_0)$ approximation].

We need to keep fluctuations into account at the macroweather scale. A phenomenological way (Hasselmann's proposal) is to replace the model above by

$$dT_{mw}(t) = \overline{g}\left(T_{mw}(t), q(t)\right) dt + \sqrt{\epsilon}\sigma\left(T_{mw}(t), q(t)\right) \circ dW(t),$$

for a suitable "volatility" σ (Stratonovich integral $\circ$ looks more appropriate). In Ref. 21, heuristic justifications are given, inspired, for instance, the random displacements of a Brownian particle in a fluid of molecules (which on their own are subject to a deterministic fast dynamics, coupled with the slow deterministic dynamic of the bigger particle). The Bremen School on Random Dynamical Systems and other research groups explored for some time rigorous justifications for this proposal, but a final answer is not known, see, for instance, Refs. 23 and 24. However, the observation of temperature time series at the timescale of month-year clearly shows some form of stochasticity and, thus, Hasselmann's proposal looks very appealing.

For our purposes below, adhering to Hasselmann's proposal is essential, since our results are the consequence of random perturbations of a nonlinear system representing climate dynamics at the macroweather timescale, namely, a stochastic version of the EBM. Random perturbations are often accepted just based on the generic justification of an unknown coupling with other segments of the physical system (which at the end of the story is the reason also here, namely, the coupling with the fast variables) but Hasselmann's proposal is a more precise explanation.

Let us, however, advise the reader that we shall start, in our example below, from a stochastic PDE for the temperature macroweather-scale, given *a priori*, not derived precisely from the weather scale as described above. We want to concentrate on the consequences of particular nonlinearities. Our model will have a simplified form

$$dT_{mw}(t) = \overline{g}\left(T_{mw}(t), q(t)\right) dt + \sqrt{\epsilon}\sigma\, dW(t)$$

with constant σ.

E. Macroweather and climate

As announced at the end of Subsection II E, our investigation starts from an equation of the form (stochastic differential equation

or SPDE)

$$dT(t) = \overline{g}\left(T(t), q(t)\right) dt + \sigma\, dW(t), \tag{1}$$

$q(t)$ slowly varying,

where we skip the subscripts but keep in mind that it is a macroweather model, we have skipped the factor $\sqrt{\epsilon}$ but we shall choose a small diffusion coefficient σ, and the nonlinear function $\overline{g}$ will be chosen by means of typical arguments related to EBMs. The slowly varying function $q(t)$ will describe the effect, in the model, of slowly varying CO_2-concentration, appreciated on a timescale of dozens of years.

The climate is a collection of statistical information from the time series of this model. If it were an autonomous system [$q(t)$ equal to a constant], we would invoke invariant measures. Due to the time change in $\overline{g}$, we have to use the formalism of time-varying invariant measures. However, at the simulation level, we approximate this time-varying system by an adiabatic system parametrized by a parameter q,

$$dT(t) = \overline{g}\left(T(t), q\right) dt + \sigma\, dW(t)$$

and investigate its invariant measures, parametrized by q. The slow change of statistics for the true non-autonomous system is mimicked by the change of statistics when the parameter q is changed.

Concerning precisely the concept of climate, let us introduce some formalism. We again limit ourselves to stochastic differential equations (SDEs) on an Euclidean space $\mathbb{R}^d$ (e.g., the space-discretization of a stochastic partial differential equation, as in our main example below) but the concepts can be widely generalized, see, for instance, Ref. 25 for a non-autonomous abstract random dynamical system framework related to the weather-climate dichotomy (that we improve hereby introducing a third level, the macroweather). Call $\mathrm{Pr}\left(\mathbb{R}^d\right)$ the set of probability measures on Borel sets of $\mathbb{R}^d$. Consider the SDE (1) on the full real line of time. Assume that $W(t)$ is a d-dimensional two-sided Brownian motion defined on a Probability space $(\Omega, \mathscr{F}, \mathbb{P})$ with expectation $\mathbb{E}$. Assume that, for the Cauchy problem on the half line $[t_0, \infty)$ with initial condition T_0 at time t_0, with arbitrary t_0 and T_0, at least weak global existence and uniqueness in law holds, and denote the solution by $T^{t_0, T_0}(t)$, $t \in [t_0, \infty)$; assume $T_0 \mapsto T^{t_0, T_0}(t)$ is Borel measurable from $\mathbb{R}^d$ to $\mathrm{Pr}\left(\mathbb{R}^d\right)$ endowed with the weak convergence of measures.

For all $t_0 < t$, we introduce the Markov semigroup $\mathscr{P}_{t_0, t}$ mapping $\mathrm{Pr}\left(\mathbb{R}^d\right)$ into $\mathrm{Pr}\left(\mathbb{R}^d\right)$ defined by the identity

$$\int_{\mathbb{R}^d} \phi\left(y\right) \left(\mathscr{P}_{t_0, t}\nu\right)\left(dy\right) = \mathbb{E} \int_{\mathbb{R}^d} \phi\left(T^{t_0, T_0}(t)\right) \nu\left(dT_0\right),$$

for every $\nu \in \mathrm{Pr}\left(\mathbb{R}^d\right)$ and every bounded continuous test function ϕ on $\mathbb{R}^d$. One can prove that

$$\mathscr{P}_{r,t}\mathscr{P}_{s,r} = \mathscr{P}_{s,t},$$
$$\mathscr{P}_{s,s} = Id.$$

Moreover, one can link the Markov operator for Eq. (1) to the Fokker–Planck equation

$$\partial_t f + \mathrm{div}\left(\overline{g}\left(\cdot, q\right)f\right) = \frac{\sigma^2}{2}\Delta f,$$

but we do not stress the rigorous results here.

The set of probability densities $\Pr\left(\mathbb{R}^d\right)$ is the state-space for the climate. In other words, any $\nu \in \Pr\left(\mathbb{R}^d\right)$ is a (possible) state for the climate. Further, fixed the times $t_0 < t$, the operator $\mathscr{P}_{t_0,t}$ defines the evolution, from t_0 to t, of the climate dynamics. Thus, we look for the climate concept inside the class of time-varying invariant measures, which are invariant under the operator defining the climate dynamics, i.e., a family

$$\{\mu_t\}_{t\in\mathbb{R}} \subset \Pr\left(\mathbb{R}^d\right),$$

such that

$$\mathscr{P}_{s,t}\mu_s = \mu_t \quad \text{for every } s \leq t.$$

Remark 2 The concept of time-dependent invariant measure $\{\mu_t\}_{t\in\mathbb{R}}$ should not be confused with any solution of the Fokker–Planck equation. Similarly to the fact that, in many cases, the invariant measure μ of an autonomous system is the limit, as $t \to +\infty$, of the law of the solution $X_t^{x_0}$ starting at time $t = 0$ from the initial condition x_0, independent of x_0, the time-dependent invariant measure μ_t is expected to be, in many cases, the limit as $t_0 \to -\infty$ of the law of the solution $X_t^{t_0,x_0}$ starting at time t_0 from x_0, independently of x_0 (property that we could call "pull-back convergence to the equilibrium").

Two simple illustrative examples are the Ornstein-Uhlenbeck equations with periodic or linear growth. For the periodic equation,

$$dX_t = -X_t\,dt + \sin(t)\,dt + dW_t,$$

the unique time-dependent invariant measure μ_t is the law, 2π-periodic of the process

$$X_t := \int_{-\infty}^{t} e^{-(t-s)}\sin(s)\,ds + \int_{-\infty}^{t} e^{-(t-s)}\,dW_s.$$

For the linear growth equation (closer to our model with CO_2 increase),

$$dX_t = -X_t\,dt + t\,dt + dW_t,$$

the unique time-dependent invariant measure μ_t is the law of the process

$$X_t := \int_{-\infty}^{t} e^{-(t-s)}s\,ds + \int_{-\infty}^{t} e^{-(t-s)}\,dW_s.$$

Under suitable assumptions for the stochastic equations, there are results of existence (easy, in particular, relying on the existence of a compact global attractor) and also uniqueness (more difficult) for such invariant families. This part of the theory is in progress. When the invariant measure $\{\mu_t\}_{t\in\mathbb{R}}$ is unique, we call it "the climate."

When uniqueness does not hold or it is not known, the idea could be to look for families μ_t not only invariant but also with additional properties of interest for physical sciences or other reasons. A typical one could be a pull-back version of "convergence to equilibrium":

$$\mu_t = \lim_{s\to-\infty} \mathscr{P}_{s,t}\lambda, \tag{2}$$

where λ is a "natural" measure, as a rotation invariant centered Gaussian measure on $\mathbb{R}^d$. For simplicity of understanding, the reader

can assume that there is one and only one invariant family μ_t or one selected by the pull-back property above.

If $q(t)$ varies very slowly, we expect that also μ_t varies accordingly, and thus an adiabatic approach to the numerical computation of μ_t is reasonable, as already remarked above.

It is crucial to emphasize the following point. We believe that viewing climate as a time-dependent invariant measure, constructed in the pull-back sense, is not only a rigorous definition but also a physically meaningful one. Indeed, the current climate is the result of a long-term evolution that began in the distant past, where the dependence on the initial condition has been lost. This idea, together with the application to geophysical science of concepts from dynamical systems theory, developed in the 1990s,[26,27] began gaining traction approximately 15 years ago.[28,29]

III. ENERGY BALANCE MODELS

A. The macroweather timescale and the global mean temperature increase due to carbon dioxide concentration

EBMs are elementary climate models where, in the simplest form, the temperature of the planet evolves according to the balance of the radiation absorbed and emitted by the Earth.[7,10–13] Their ability to capture the essential dynamics of Earth's climate system while remaining computationally tractable makes EBMs valuable tools for understanding a wide range of climate phenomena, from the onset of ice ages to the impacts of greenhouse gas emissions on global temperatures.[30,31] There exists a spectrum of complexity for this kind of model, starting from the zero-dimensional (0D) case, moving to the one-dimensional (1D) case, and arriving at higher-dimensional models.[16] Before delving into the details of our 1D EBM with space heterogeneous radiation balance, we illustrate (i) why an EBM has a macroweather timescale, and (ii) why an increase in CO_2 concentration in a stochastic 0D EBM leads to an increase in GMT, but not the variance of the solution.

First, we consider a 0D EBM for the global mean temperature $T = T(t)$ which, given a positive initial condition T_0, is an ODE of the form

$$C\frac{dT}{dt} = Q_0\beta + q - A - B \cdot (T - 273), \tag{3}$$

$$T(0) = T_0.$$

In this model, the radiation emitted R_e by the planet is assumed, according to the Budyko empirical radiation formula,[10] of the form

$$R_e(T) = A + B \cdot (T - 273) - q,$$

where A, B are positive constants that can be derived by a best-fit estimate with real data observations; $C > 0$ denotes the heat capacity per square meter, while Q_0 and β are, respectively, the global mean radiation and coalbedo. Lastly, the additive parameter $q > 0$ is the effect of CO_2 concentration on the radiation balance.[16,31,32] Denoting by T_* the unique stable fixed point of the model, i.e.,

$$T_* = \frac{Q_0\beta - A + q}{B} + 273,$$

20 September 2024 07:18:12

the solution of Eq. (3) is given by

$$T(t) = T_* + (T_0 - T_*)\, e^{-t/\tau_0},$$

where $\tau_0 = C/B$ is the relaxation time, i.e., the timescale at which a deviation from the equilibrium temperature is reabsorbed. Considering an all-land planet, it is reasonable to consider the heat capacity as half the heat capacity at a constant pressure of the column of dry air over a square meter, as pointed out in Ref. 16, leading to

$$C = 5 \cdot 10^7 \, \text{J K}^{-1} \, \text{m}^{-2}.$$

On the other hand, the satellite data suggest[16,33]

$$B = 1.90 \, \text{W m}^2 \, \text{K}^{-1}.$$

This leads to a relaxation time of the other of one month, as

$$\tau_0 = \frac{C}{B} = 2.63 \times 10^7 \, \text{s} \approx 30 \, \text{days}.$$

It is worth pointing out that the hypothesis of an all-land planet is a huge simplification of reality. Indeed, the Earth's system has various components capable of storing heat efficiently, each with its own unique capacity.[7] The value for C we have considered corresponds to the capacity of the atmospheric column. But, even considering a planet with a mixed-layer only ocean, the heat capacity would be 60 times larger (see Ref. 16), i.e., in the order of a few years, thus remaining in the macro weather timescale.

    Second, we force the model with a stochastic noise modeling the effect of fast terms with respect to the slow radiation balance terms of Eq. (3). Denote by $(W_t)_{t\geq0}$ a Brownian motion, and consider the SDE given by

$$C dT_t = \left(Q_0\beta + q - A - BT_t\right) dt + \sigma \, dW_t,$$
$$T(0) = T_0, \tag{4}$$

where $\sigma > 0$ is the noise intensity. Denoting by $\tilde{A} = Q_0\beta + q - A$, the solution can be explicitly written, using a variation of parameters technique[34] as

$$T_t = T_0\, e^{-t/\tau_0} + \frac{\tilde{A}}{\tau_0}\left(1 - e^{-t/\tau_0}\right) + \sigma \int_0^t e^{-(t-s)/\tau_0}\, dW_s.$$

The solution is a Gaussian process with a mean value

$$\mathbb{E}\left[T_t\right] = T(0)\, e^{-t/\tau_0} + \tilde{A}\left(1 - e^{-t/\tau_0}\right), \tag{5}$$

and variance

$$Var(T_t) = Var\left(\frac{\sigma}{C}\int_0^t e^{-(t-s)/\tau_0} ds\right) = \frac{\sigma^2}{C^2}\int_0^t e^{-2(t-s)/\tau_0}\, ds$$
$$= \frac{\sigma^2}{2BC}\left(1 - e^{-2t/\tau_0}\right). \tag{6}$$

Further, the stochastic EBM in Eq. (4) has a unique Gaussian invariant measure $\nu \sim \mathcal{N}(\mu_\nu, \sigma_\nu^2)$, whose mean μ_ν and variance σ_ν^2 can be obtained taking the limit for the time that tends to infinity in Eqs. (5) and (6), leading to

$$\mu_\nu = \tilde{A} = \frac{Q_0\beta + q - A}{B}, \quad \sigma_\nu^2 = \frac{\sigma^2}{2BC}.$$

Thus, a change in the CO_2 concentration leads to a change in the mean value of the climate, i.e., the invariant measure, but not in

its variability. Usually, the variability increase results from a critical transition, such as a saddle-node bifurcation, which arises in the model. This is the concept of bifurcation-induced tipping point, which leads to the critical slowing down behavior of the system, resulting in an increase in variance and autocorrelation close to the bifurcation point.[2,3,5,6] However, the presence of a bifurcation point for the global scale climate is questionable, and the presence of bistable regimes for climate components, sometimes called tipping elements such for the Atlantic meridional overturning circulation or polar ice sheets, is localized in space. For all these reasons, in Sec. III B, we will describe a new one-dimensional model with a local in-space change in the non-linear term that is able to explain the variance increase.

B. Model formulation

    In this section, we propose a 1D EBM with space-dependent radiation balance with local bistability in the outgoing radiation term. The new term does not lead to the addition of a new bifurcation in the model, even if results in a non-linear change in the global mean temperature with respect to CO_2 concentration, in comparison with a linear increase in the case of the non-space dependent emitted radiation case. However, by adding a noise component to the model, we detect an increase in fluctuations over time for those values of CO_2 concentration in which the non-linear behavior of GMT is triggered. We connect the increase in fluctuations over time, that we denote *time variance*, to a local (in space) notion of *relaxation time*. The latter indicator in a sense gives information about the local stability of a space point for, in our case, a global stable temperature configuration.

    The main characteristics of a 1D EBM are that the temperature $u = u(x,t)$, depending on time t and space $x = sin(\phi)$, where $\phi \in [-\pi/2, \pi/2]$ denotes latitude, are that it evolves according to the diffusion of heat, and the planet energy balance.[10,11,13,15] Our model, which is an extension of the one considered in Ref. 32, assumes that the temperature u satisfies the non-linear parabolic partial differential equation

$$C_T \partial_t u = \partial_x\left(\kappa(x)u_x\right) + R_a(x,u) - R_e(x,u;q), \ x \in [-1,1], t \geq 0,$$
$$u(x,0) = u_0(x), \quad x \in [-1,1], \tag{7}$$
$$u_x(-1,t) = u_x(1,t) = 0, \quad t \geq 0.$$

The heat capacity $C_T = 5 \times 10^{-7} \, \text{J K}^{-1}\,\text{m}^{-2}$ is considered uniform over the whole planet, which we assume is an all-land planet, as the one presented at the beginning of Sec. III. The PDE is a reaction–diffusion type.[35,36] Classical results can be used to prove the global existence and uniqueness of the solution, given a regular initial condition.[35] Further, it can be proved that $[0, +\infty)$ is an invariant region in the sense of Ref. 36, as pointed out in Ref. 32. In the following, we are going to describe the terms governing its time evolution, while the values of the constants appearing in the parametrizations can be found in Table I.

    In scientific modeling, heat diffusion is often depicted assuming the planet as a thin shell. This leads to a non-constant diffusion coefficient of the form $\kappa(x) = D \cdot (1 - x^2)$, with $D > 0$, where the term $1 - x^2$ arises due to the spherical setting.[16] However, this

TABLE I. Parameters and constants appearing in the 1D EBM (7).

Symbol	Meaning	Value
D	Diffusivity constant	0.45
$\hat{Q}_0$	Mean solar radiation	341.3 W m^{-2}
ε_0^{pl}	Emissivity at the poles	0.61
ε_0^{eq}	Emissivity at the equator	0.478
σ_0	Boltzmann's constant	$5.67 \cdot 10^{-8} \text{ W m}^{-2} \text{ K}^{-1}$
α_1	Ice albedo	0.7
α_2	Water albedo	0.289
K	Constant rate—albedo parametrization	0.1
K^{SGE}	Constant rate—SGE parametrization	0.1
u_{ref}	Reference temperature—albedo parametrization	273 K
u_{ref}^{SGE}	Reference temperature—SGE parametrization	303.2 K
C_T	Heat capacity	$5 \times 10^7 \text{ J m}^{-2} \text{ K}^{-1}$

choice introduces difficulties for the mathematical treatment, resulting in degenerate problems.[37,38] For instance, proving the existence of steady-state solutions requires the use of weighted Sobolev spaces. To address this issue, we introduce a simplifying perturbation that removes the singularity at the border.[32] We consider the diffusion function given by

$$\kappa(x) = D \cdot \left(1 - x^2\right) + \delta(x),$$

with $D = 0.3$ and $\delta \in C^\infty(-1, 1)$, $\delta(x) = 0$ if $|x| \leq \eta$, δ even and non-decreasing in $(0, 1)$. The radiation absorbed by the planet, denoted as R_a, is the product of a spatially dependent solar radiation function $Q_0(x) = \hat{Q}_0 \cdot (1 - x^2)$, where $\hat{Q}_0 > 0$, and a temperature-dependent co-albedo $\beta = \beta(u)$. The co-albedo $\beta(u) = 1 - \alpha(u)$, where α is parameterized by a smooth, non-increasing, bounded function[31,32]

$$\alpha(u) = \alpha_1 + \frac{\alpha_2 - \alpha_1}{2} \cdot \left[1 + \tanh\left(K \cdot \left(u - u_{ref}\right)\right)\right], \quad (8)$$

with $0 < \alpha_1 < \alpha_2 < 1$, α_1 denotes ice albedo, α_2 denotes water albedo, $u_{ref} = 275$ K, and K is a parametrization constant.

Third, we describe the modeling of the radiation emitted R_e, which is the main innovation of our model. Local bistability in the Outgoing Longwave Radiation (OLR) may arise in tropical regions due to a positive feedback loop involving surface temperature and moisture. This feedback, above a threshold of sea level pressure and GHG concentration, causes the atmosphere to become optically thick, thus reducing OLR.[9]

To model this effect, we choose a space-dependent, latitude-symmetric Outgoing Longwave Radiation (OLR) of the form

$$R_e(x, u; q) = q + |x| R_e^{pl}(u) + (1 - |x|) R_e^{eq}(u), \quad (9)$$

where R_e^{pl} and R_e^{eq} denote, respectively, the OLR at the pole and the equator. The convex combination between R_e^{pl} and R_e^{eq} (Fig. 3) shows the space-dependent OLR R_e, using different colors to represent
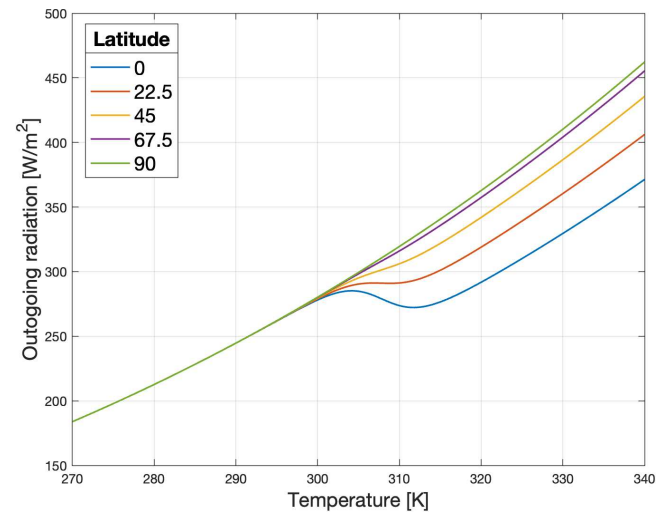

FIG. 3. Representation of the Outgoing Longwave Radiation (OLR) $R_e = R_e(x, u; q)$ in Eq. (9) for $q = 0$. Different colors are used to represent the dependence on the space. At the tropics, the OLR presents the bistability due to the super-greenhouse effect shown in Fig. 2. The bistable regimes progressively disappear as the space point moves to the poles, where the Stefan–Boltzmann law in Eq. (10) is applied to parametrize OLR.

distinct latitude points. We define them as

$$R_e^{pl}(u) = \varepsilon_0^{pl} \sigma_0 u |u|^3, \quad (10)$$

where ε_0 is the emissivity constant and σ_0 is the Stefan–Boltzmann constant. On the other hand, at the poles, we reproduce the super-greenhouse effect by considering

$$R_e^{eq}(u) = R_e^{pl}(u)g(u) + (1 - g(u))\varepsilon_0^{eq}\sigma_0 u|u|^3, \quad (11)$$

where g is a smooth transition function of the form

$$g(u) = \frac{1}{1 + e^{\left(u - u_{ref}^{SGE}\right)K^{SGE}}},$$

where $u_{ref}^{SGE} = 303.2$ K and $K^{SGE} = 0.36$ are, respectively, a reference temperature and a constant in the transition velocity involved in the SGE parametrization. Further, $\varepsilon_0^{eq} < \varepsilon_0^{pl}$ is an emissivity constant at the equator taking into account the OLR reduction due to the SGE. Note that the OLR at the poles and at the equator in Eqs. (10) and (11) has been defined, just for mathematical convenience, in the physically meaningless range of negative Kelvin temperature.

Lastly, the additive positive parameter q models the effect of CO_2 concentration on the energy budget.[31,39] A higher q leads to lower radiation emitted back to space from the surface. We emphasize the reason behind considering a constant value for the CO_2 parameter q. Greenhouse gas concentration can be regarded as constant at a macroweather, i.e., monthly, timescale by avoiding seasonality insertion since it evolves on a much larger timescale. For instance, the CO_2 concentration has increased by around 47% from 1850 to 2020, moving from 284 parts per million (ppm) to 412 ppm.[40] In a first approximation, we assume that the spatial

distribution of greenhouse gases is uniform over the globe. This assumption, although no longer the state of the art, was widespread at the turn of the century and is based on the well-mixing property of GHG. This means that since most GHGs, such as CO_2, have a large lifetime, many studies have been conducted using global average values for the spatial distribution.[1,39,41]

C. Deterministic properties of the model

In this section, we describe the deterministic properties of our model as the number of steady-state solutions and their stability. The new feature of our model is the rise of a strong non-linear increase in GMT with respect to the greenhouse parameter q, in the proximity of the model configuration describing the actual climate of the Earth.

In general, in dynamical system theory, huge information is given by the study of the steady-state solutions of the model, which are, in a sense, the long-time behavior solutions. More specifically, in our model, these solutions consist of the non-negative solutions $u = u(x)$ of the following elliptic PDE:

$$0 = \left(\kappa(x)u'\right)' + R_a(x,u) - R_e(x,u;q),$$
$$0 = u'(-1) = u'(1). \tag{12}$$

A common way to prove the existence of at least one stable steady-state solution involves a variational approach by studying the minimization problem

$$\inf\left\{F_q(u) \mid u \in H^{1,2}(-1,1),\ u \geq 0\right\}, \tag{13}$$

where

$$F_q(u) = \int_{-1}^{1} \mathscr{R}(x,u(x))\,dx + \frac{1}{2}\int_{-1}^{1}\left[\kappa(x)u'(x)\right]^2\,dx, \tag{14}$$

with $\partial_u\mathscr{R} = R_e - R_a$ and $H^{1,2}(-1,1)$ denoting the Sobolev space of order 1 and exponent 2.[12,42–44] Applying the results of Ref. 32, Theorems 1 and 3, it is possible to gain information about the existence and uniqueness of a steady-state solution.

Proposition 1

(i) *There exists a unique minimizer $u_* \in C^\infty([-1,1])$ of the variational problem (13). Further, u_* solves the elliptic problem (12) and it is stable for the dynamics of the 1D EBM (7).*

(ii) *The map $q \mapsto \frac{1}{2}\int_{-1}^{1} u_*(x)ds$ is non-decreasing.*

Note how the second part of the previous result gives qualitative information on the behavior of the GMT. Furthermore, if the diffusion coefficient is sufficiently large and the 0D EBM, obtained by removing the diffusion term and averaging in space the radiation balance, is bistable, it can be rigorously proven the existence of a second stable steady-state solution and a third unstable one.[32]

Given the non-linear nature of the problem, a rigorous demonstration of all properties of the model is not always possible. In this case, the problem can be overcome by using numerical simulations. In particular, for each fixed q, we numerically simulated the solutions of Eq. (12). As q varies, we obtained, according to the large literature on this kind of model, that there can be either 1 or 3 stationary solutions. In the former case, the solution is stable. In the latter case, two solutions are stable, one describing a "snowball" configuration u_S for Earth's temperature with ice all over its surface.

The other describes a warm climate u_W, similar to the one in which we are living. Additionally, an unstable solution u_M, whose average global mean temperature (GMT) lies between the GMT of u_S and u_S, also arises. See Fig. 4(a) for a graphical representation of the steady-state solutions in the bistable case.

In general, proving theoretically the results for such kinds of models is non-trivial due to the presence of nonlinear terms in the energy budget parametrization. The bifurcation diagram of the model in the $(q, \bar{u}_*)$ plane, where u_* denotes a solution of the elliptic PDE, and $\bar{u}_* = \frac{1}{2}\int_{-1}^{1} u_*(x)\,dx$ is its GMT, is depicted in Fig. 4(b). We highlight how the addition of a space-dependent OLR with tropics bistability does not introduce a new bifurcation. Thus, no new steady-state solutions are added or the stability of the already existing ones is altered. However, as highlighted in Fig. 4(c), a strong non-linear behavior of the GMT for the warm solution u_W appears for the value of q in the neighborhood of $q \approx 11.3$, a thing that does not happen if we remove the bistability in R_e.[32] We aim to focus on that phenomenon, when a noise component, describing the weather effect, is added to the model. This is the main topic of Secs. III D and III E.

D. Stochastic properties of the model

As discussed in the previous paragraphs, the EBM presented in this work corresponds to a macroweather timescale. However, as far as it has been introduced, it lacks in taking into account the effect of fast components of Earth's system, such as atmospheric pressure, wind, and precipitation. In the literature, this has been achieved elementary by adding a stochastic term, such as white noise, to the radiation budget.[21,45–47] Note that this addition is necessary to describe the increase in the frequency of rare events. In fact, while a deterministic EBM is useful for obtaining information on global mean temperature, it is not able to investigate fluctuations around it due to all phenomena, such as weather, not included in the radiation balance of the model.

We consider $H = L^2(-1,1)$ and the stochastic EBM given by

$$du_t = [Au_t + R(x,u_t)]\,dt + \sigma\,dW_t,$$
$$u_{|t=0} = u_0, \tag{15}$$

where $(W_t)_t$ denotes the cylindrical Wiener process on H, $u_0 \in H$ is a non-negative initial condition, and $A : D(A) \to L^2(-1,1)$ is the operator

$$D(A) = \left\{u \in H^2(-1,1) \mid u'(-1) = u'(1) = 0\right\},$$
$$Au = \left(\kappa(x)u'\right)'. \tag{16}$$

We would like to apply the invariant measure theory for gradient systems to deduce the existence and uniqueness of an invariant measure and its explicit formula. This cannot be applied to the operator A since it is invertible on $L^2(-1,1)$. For this reason, we consider the operator

$$\tilde{A} = \lambda Id - A, \tag{17}$$

where $\lambda > 0$ is a positive constant. By exploiting the Sturm–Liouville theory, it can be proved that $-\tilde{A}$ is a self-adjoint, negative definite operator, with eigenvalue $0 < \lambda_1 < \lambda_2 < \cdots$, such that the trace of
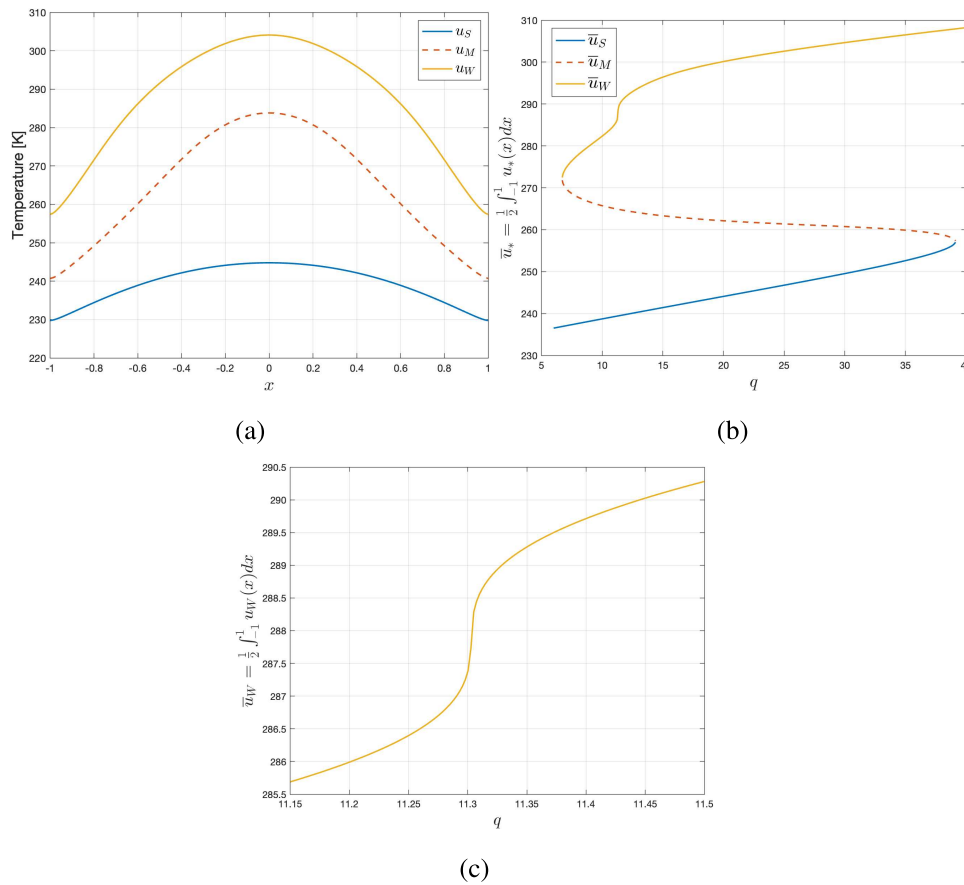
FIG. 4. (a) Steady-state solutions for the 1D EBM (7) for $q = 11.3$. Solid lines denote stable solutions, and dotted lines denote unstable solutions. The snowball solution u_S is plotted in blue, the middle solution u_M in red, and the warm solution u_W in yellow. (b) Bifurcation diagram in the $(q, \bar{u}_*)$ plane for the 1D EBM (7), where u_* denotes steady-state solutions and $\bar{u}_* = \frac{1}{2}\int_{-1}^{1} u_*(x)\,dx$ is its global mean temperature (GMT). The S-shaped bifurcation diagram is characterized by the two classical saddle-node bifurcations around $q \approx 7$ and $q \approx 38$, and a non-linear (with respect to q) increase in GMT around $q \approx 22$. (c) Zoom of the bifurcation diagram around $q \approx 11.3$ and u_W.

$Tr\left[\left(-\tilde{A}\right)^{\beta-1}\right] < +\infty$, for some $\beta \in (0,1)$. See Appendix B for a sketch of the proof of these facts. In this way, it is possible to deduce the following result.[20,32,48]

Proposition 2 *Let $E = C([-1,1])$. Then, there exists a unique $\mathbb{P}$-a.s. E-valued mild solution of the SPDE (15). Further, there exists a unique Gibbs invariant measure $\tilde{\nu}$, and $\tilde{\nu} \ll \tilde{\mu}$ with explicit formula*

$$\tilde{\nu}(du) = \frac{1}{Z}\exp\left(-\frac{2}{\sigma^2}\tilde{I}(u)\right)\tilde{\mu}(du), \tag{18}$$

where $\tilde{\mu} \sim \mathcal{N}\left(0, -\frac{\sigma^2}{2}\tilde{A}^{-1}\right)$ and

$$\tilde{I}_q(u) = \int_{-1}^{1}\mathcal{R}(x, u(x))\,dx - \frac{\lambda}{2}||u||_2^2.$$

We remark that the invariant measure $\tilde{\nu}$ is the object, in our context of stochastic EBM, that in Sec. II E has been taken as the definition of climate. Then, it is worth pointing out the link between

the invariant measure $\tilde{\nu}$ and the functional F_q building up the variational problem (13). Indeed, at least formally, we can write the Gaussian measure $\tilde{\mu}$ as

$$\tilde{\mu}(du) = \frac{1}{Z_1}\exp\left(-\frac{1}{2}\langle\mathcal{Q}^{-1}u, u\rangle\right)\text{``}du\text{''},$$

where Z_1 is a normalization constant, $\mathcal{Q} = -\frac{\sigma^2}{2}\tilde{A}^{-1}$ is the covariance operator of $\tilde{\mu}$, $\langle\cdot,\cdot\rangle$ denotes the scalar product on $H = L^2(-1,1)$, and "du" is the formal notation for the Lebesgue measure on H. By an integration of parts, we deduce

$$-\frac{1}{2}\langle\mathcal{Q}^{-1}u, u\rangle = -\frac{2}{\sigma^2}\left(\frac{\lambda}{2}||u||_2^2 - \frac{1}{2}\langle\kappa(x)u', u'\rangle\right).$$

Hence, substituting back the formal expression for $\tilde{\mu}$ in Eq. (18), we conclude

$$\tilde{\nu}(du) \propto \exp\left(-\frac{2}{\sigma^2}F_q(u)\right)\text{``}du\text{''}.$$

From this expression, we can deduce two important facts. First, the invariant measure of the stochastic EBM is concentrated on the global minimum points of the functional F_q. Second, the study of $\tilde{\nu}$ and its spread depending on q is as difficult as understanding how the functional F_q changes. For this reason, in Sec. III E, we will use numerical simulation to investigate how $\tilde{\nu}$ changes, depending on the adiabatic parameter q, as CO_2 lies in the critical interval in Fig. 4(c).

E. Variance and extreme weather events increase

It is widely acknowledged that greenhouse gas emissions from human activities have led to more frequent and intense weather and climate extremes since the pre-industrial era, particularly temperature extremes.[40] Despite numerous definitions proposed to assess what constitutes an extreme event, there is currently no universally accepted definition.[49] One commonly used definition considers an extreme weather event as one that exceeds a predefined threshold for a climate variable.

As it is well understood that such occurrences become more likely as the variance of that climate variable increases, we consider the time variance as a proxy indicator of extreme weather events for our EBM setting. As explained in Sec. III D, an explicit formula for the invariant measure of the stochastic EBM (4) exists. However, due to the presence of a non-linear term inside the Gibbs factor in Eq. (18), obtaining theoretical information is challenging. Thus, we rely on numerical simulations to capture the behavior of the variance.

Specifically, given a fixed value of $q > 0$ and the warm steady-state solution $u_W = u_W^{(q)}$, we numerically integrate the stochastic PDE,

$$C_T \partial_t u = \partial_x (\kappa(x) u_x) + R_a(x, u) - R_e(x, u; q) + \sigma \, dW_t,$$
$$(x, t) \in [-1, 1] \times [0, T],$$
$$u(x, 0) = u_W(x), \quad x \in [-1, 1], \tag{19}$$
$$u_x(-1, t) = u_x(1, t) = 0, \quad t \in [0, T].$$

The simulation runs for $T = 500$ years to capture the properties of the invariant measure around the warm climate u_W, and we chose a noise intensity $\sigma = 0.2$. The finite difference method applied to simulate the equation is detailed in Appendix A. Here, we describe what we mean by variance, its properties detected by numerical experiments, and our observations.

Given a space point $x \in [-1, 1]$ and a realization $\omega \mapsto u(\omega)$ of the solution of Eq. (19), we consider the variance of the process $t \mapsto u_t(x, \omega) = u(x, t)$. We denote the numerical approximation of the solution by $U = (u_{ij})_{ij}$, where $u_{ij} = u(x_i, t_j)$, and $(x_i)_{i=1,...,n}$ and $(t_j)_{j=1,...,m}$ represent the spatial and temporal meshes, respectively, over the domain $[-1, 1]$ and $[0, T]$. The time-variance is calculated as

$$\sigma_t^2(x_i) = \frac{1}{m} \sum_{j=1}^{m} (u_{ij} - \bar{u}_i)^2,$$

where $\bar{u}_i = \frac{1}{m} \sum_{j=1}^{m} u_{ij}$. Figure 5(a) illustrates the time-variance indicator, with different colors representing different values of the parameter q.

We observe two distinct behaviors of the variance. First, depending on q, there is an increase in σ_t^2, peaking around $q \approx 11.3$, followed by a decrease. This peak corresponds to the q value that results in the largest increase in GMT, as shown in Fig. 4(c). Second, as expected, for a given value of q, the spatial profile of σ_t^2 is symmetric with respect to $x = 0$. Additionally, three local maximum points emerge one at $x = 0$ and the others at $|x| \approx 0.8$. Our interpretation is that σ_t^2 identifies the highest fluctuating regions as those where the freezing water temperature is crossed (sub-arctic regions, $|x| = 0.8$), or where the SGE triggers bistability (tropical areas, $x = 0$).

To support this interpretation, it is useful to introduce the local stability indicator

$$\gamma(x) = \partial_u R(x, u_W(x)),$$

where $R(x, u) = R_a(x, u) - R_e(x, u; q)$. If the model were a simple Ordinary Differential Equation (ODE) without the coupling diffusion term, $\gamma(x)$ would be, up to a positive constant depending on C_T, the eigenvalue obtained by linearizing the reaction term around the stable steady-state temperature $u_W(x)$. Positive values of $\gamma(x)$ indicate local instability, while negative values indicate stability if the diffusion term is removed. Figure 5(b) presents the local stability indicator γ, with colors denoting different values of the parameter q. Notably, there is a clear relationship between time-variance and the local stability indicator: regions with high time-variance σ_t^2 coincide with areas of positive γ. This explains the spatial profile of σ_t^2 for a fixed value of q.

The reason for $\gamma(x) > 0$ at some points is due to the presence of the diffusion term. If $\kappa \equiv 0$, then u_W is not a minimizer of F_q, but instead solves the problem

$$u_W(x) = \underset{u \geq 0}{\arg\min} \, \mathscr{R}(x, u), \tag{20}$$

where $\partial_u \mathscr{R} = R_e - R_a$. Here, $\partial_u \mathscr{R}_{|(x, u_W(x))} = 0$, and since $u_W(x)$ is a minimum point, it follows $\partial_u^2 \mathscr{R}_{|(x, u_W(x))} = \partial_u R_{|(x, u_W(x))} \leq 0$. But with $\kappa(x) > 0$, $u_W(x)$ no longer satisfies Eq. (20), but instead is a minimizer of F_q, where the diffusion term appears in the second term on the right-hand side of Eq. (14). This term, which intuitively minimizes the temperature gradient, allows for some points to fluctuate around a mean value that would be unstable if $\kappa \equiv 0$.

To understand why, given $x \in [-1, 1]$, the map $q \mapsto \sigma_t^2(x) = \sigma_t^{2,(q)}(x)$ increases until around $q \approx 11.3$ and then decreases, we offer the following explanation. As q increases, the temperature $u_W(x)$ of the warm climate increases, as can be checked by numerical simulations and partially understandable from Proposition 1. This leads the temperature, especially in the tropical area, to approach the region where instability due to the SGE arises. Once the tropical temperature surpasses this region, the instability, and thus the variance, decreases. We support our statements as follows.

(i) Figure 6 shows how the steady-state solution $u_W^{(q)}$ approaches unstable areas, defined by points (x, u) where $\partial_u R(x, u) > 0$. For $q_1 = 11.21$, $q_2 = 11.28$, and $q_3 = 11.4$, the map $(x, u) \mapsto \partial_u R(x, u_W(x))$ is presented, with the curve $x \mapsto (x, u_W(x), \partial_u R(x, u_W(x)))$ depicted in red. When the time variance peaks (i.e., $q = q_2$), the steady-state solution values around the equator are close to the local maximum of $\partial_u R$, approximately close to $(x_M, u_M) = (0, 305)$. For $q = q_1$ and $q = q_3$, the equatorial steady-state value is smaller and larger than u_M, respectively.
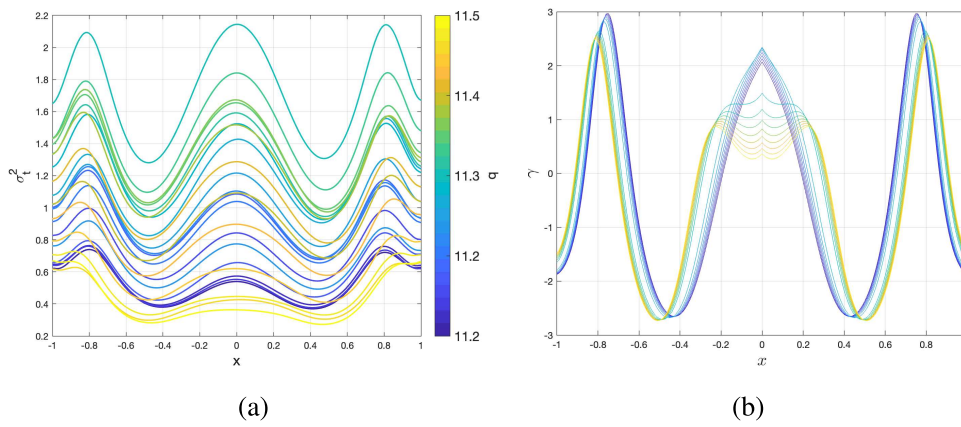
20 September 2024 07:18:12

FIG. 5. Indicators for the stochastic 1D EBM (19) over the time interval $[0, T]$, with $T = 500$ years. (a) Time-variance indicator σ_t^2. Different colors represent different values of q for which the stochastic 1D EBM is simulated. (b) Local stability indicator γ, using the same color scheme as in subfigure (a).
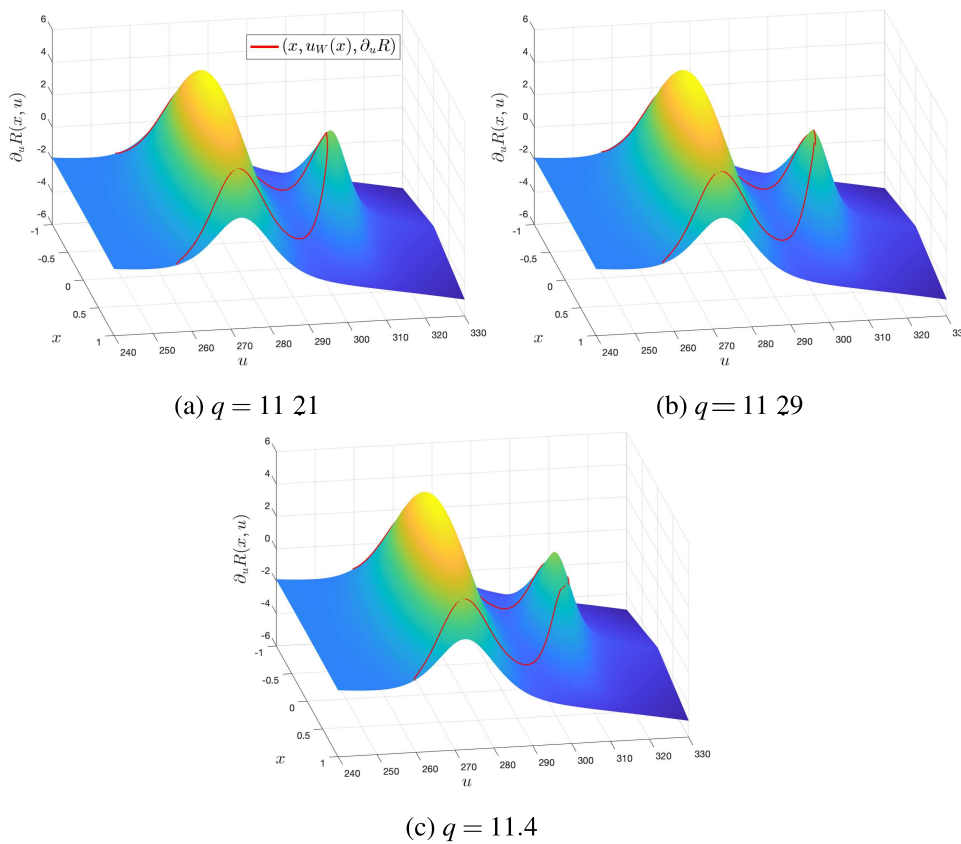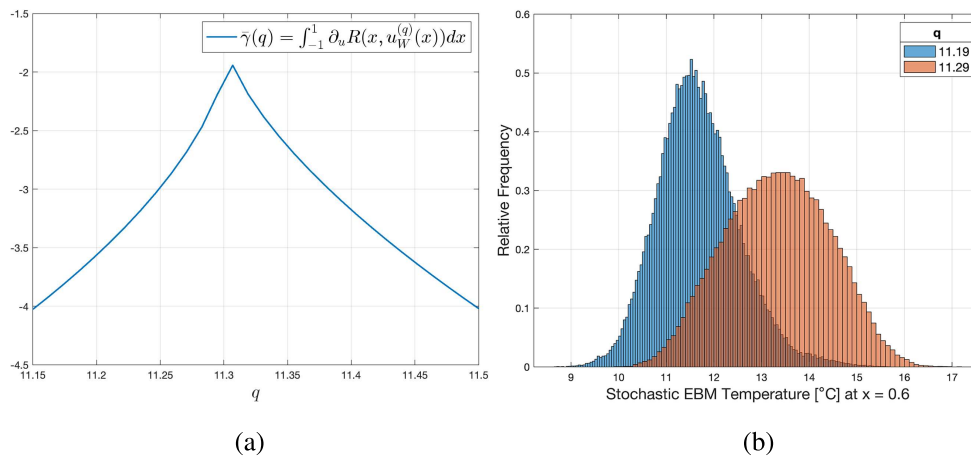

(a) $q = 11\,21$

(b) $q = 11\,29$

(c) $q = 11.4$

FIG. 6. Plot of the map $(x, u) \mapsto \partial_u R(x, u)$ and the curve $x \mapsto (x, u_W(x), \partial_u R(x, u_W^{(q)}(x)))$ in red, for different values of q.

FIG. 7. (a) Average local stability indicator $\bar{\gamma}(q) = \int_{-1}^{1} \partial_u R(x, u_W^{(q)}(x)) dx$. It increases, peaks around $q \approx 11.3$, and then decreases. (b) Histogram of the distribution of the solution of $t \mapsto u(\bar{x}, t)$ for the stochastic EBM (19) for $q = 11.2$ (blue) and $q = 11.3$ (red), at $\bar{x} = 0.6$.

(ii) We consider the local mean stability indicator

$$\bar{\gamma}(q) = \int_{-1}^{1} \gamma(x)\, dx = \int_{-1}^{1} \partial_u R(x, u_W^{(q)}(x))\, dx.$$

Its plot is shown in Fig. 7(a). Although providing only average information, it exhibits behavior qualitatively similar to that of σ_t^2 for each fixed value of x, peaking around $q \approx 11.3$.

Finally, we show the distribution of the solution $u(x, t)$ of the stochastic 1D EBM (4) for the fixed space point $x = 0.6$ (similar results are observed for different space points). Figure 7(b) shows the distribution as a histogram, comparing two distinct values of q. Blue depicts the results for $q = 11.2$, while red shows $q = 11.3$. From the plot, we deduce that our model captures the shift in the mean value and the increase in variance, correlating with the IPCC schematic climate change reproduction in Fig. 1 and weather observations in Modena in Fig. 2(a).

IV. CONCLUSIONS

In the first part of this work, we have presented a non-autonomous framework to describe the scale separation between weather, macroweather, and climate. According to Hasselmann's proposal, weather is conceptualized as arising from a set of deterministic equations, describing variables such as temperature on a fast timescale, typically from an hour to one day. Macroweather, on the other hand, encompasses variations that are neither as short-term as weather nor as long-term as climate. We assume that temperature on a macroweather timescale satisfies a stochastic equation, reflecting the most original aspect of Hasselmann's work. Additionally, at the macro weather timescale, we include a non-autonomous term to model the atmospheric CO_2 concentration, which evolves on a timescale of years. Finally, we identify climate with the invariant measure arising from the stochastic equation at the macro weather level.

In the second part, we have introduced a new 1D EBM on a macroweather timescale, which can predict the increase in the number of extreme weather events associated with climate change. The novelty of our model relies on the parametrization of the non-linear space-dependent radiation budget. Indeed, we have inserted the presence of the SGE, a phenomenon typical of tropical areas that may lead to an instability in the OLR. Our model includes a non-autonomous term $q = q(t)$, that in light of the first part, we have considered constant, that is the effect of the CO_2 concentration on the radiation balance. We have recalled the basic mathematical properties of our model, such as the existence of steady-state solutions, using also numerical simulations. Also, we have shown how the GMT of the steady-state solution increases with increasing CO_2 concentration. Third, we have the stochastic version of our 1D EBM, obtained by perturbing our model with an additive space-time white noise. Being in the class of stochastic reaction–diffusion SPDE, it is possible to write explicitly the invariant measure as a Gibbs one. However, the presence of the non-linearity arising from the radiation budget prevents us from deducing more information from the invariant measure.

The most important results of our work are presented in Sec. III E. There, we have exploited numerical simulations to study the changes in the invariant measure as the CO_2 concentration increases. To obtain this, we have performed numerical integration of the stochastic 1D EBM on a time interval of 500 years and with the initial condition the warm steady-state solution u_W of the deterministic 1D EBM, changing only q in different runs of the simulation. Given q, for each space point $x \in [-1, 1]$, we associate the extreme weather event frequency with the time variance $\sigma_t^2(x)$ of a trajectory of the stochastic 1D EBM at point x. We explain the spatial behavior of $\sigma_t^2(x)$, which presents two local maximum points for $x \approx \pm 0.8$ and one for $x = 0$, combining heuristic reasoning with empirical indicators. The informal explanation is that the presence of the diffusion term forces the stable warm stationary solution, and the oscillations around it due to noise, to take on values that are

20 September 2024 07:18:12

not stable if we were to consider the ODE obtained by removing the diffusion term. These regions of temperature, which are locally unstable, correspond to the areas where the variance σ_t^2 is highest. We also motivated the behavior of $\sigma_t^2(x) = \sigma_t^2(q)(x)$ with respect to q, at fixed x. The variance observed in this way increases to a maximum value and then decreases. This is explained by the increase in GMT due to q and the presence of the diffusion term, leading the solution of the stochastic EBM to be increasingly in, and then out of, the region of instability due to the SGE.

Lastly, we are aware that our model, although based on physical laws, is largely phenomenological. In some parts of our model, we have included simplifications of convenience, such as in the perturbation of the diffusion function, which makes the problem non-singular and thus easier to deal with mathematically; in other parts, such as in the parametrization of the space-dependent and tropic-restored OLR, we have followed the principle of simplicity. Other choices would certainly have been possible, but the elementary nature of the model leads us to avoid choices that are too fine or complex.

Concerning open questions, an important one would be understanding the correct form of the noise term. We have assumed it to be additive and without correlation in space and time. This is an extreme simplification, which allows us to deduce certain properties of the invariant measure. But already Hasselmann in his seminal work proposed a different, i.e., multiplicative, type of noise. In addition to this, understanding how the properties of the model change if more physical processes are considered, such as advection, is a problem we would like to address in the future, as well as the extension of our work to a two-dimensional setting.

ACKNOWLEDGMENTS

AUTHOR DECLARATIONS
Conflict of Interest

The authors have no conflicts to disclose.

Author Contributions

G. Del Sarto: Conceptualization (equal); Methodology (equal); Software (lead); Writing – original draft (equal); Writing – review & editing (lead). **F. Flandoli:** Conceptualization (equal); Methodology (equal); Writing – original draft (equal).

DATA AVAILABILITY

APPENDIX A: NUMERICAL SCHEME

In this section, we describe the numerical method adopted to approximate the solutions of the stochastic PDE (19). We used an implicit Euler-Maruyama method, which is a small modification of the semi-implicit Euler-Maruyama method presented in Ref. 51, Sec. 10.5.

First, it is worth recalling that the numerical experiments presented in Sec. III E are all performed for a fixed value of q, and using $u_W = u_W^{(q)}$ as initial condition of the parabolic stochastic problem (19). The steady-state solution u_W solves the elliptic problem (12). To numerically approximate it, we have applied the same finite difference scheme described in Ref. 32, Appendix A.

Second, we move to describe the numerical method for the parabolic problem. We denote by $R(x, u; q) = R_a(x, u) - R_e(x, u; q)$ the non-linear radiation budget, and the underline notation to denote a vector (e.g., $\underline{y} \in \mathbb{R}^4$). We consider two uniform meshes for the spatial domain $[-1, 1]$ and the time domain $[0, T]$, i.e.,

$$x_i = -1 + i\Delta x, \quad i = 0, \ldots, n, \quad \Delta x = \frac{2}{n}$$

and

$$t_j = j\Delta t, \quad j = 0, \ldots, m, \quad \Delta t = \frac{T}{m} = \frac{500}{m}.$$

The number of points in the space and time mesh, respectively, $n + 1$ and $m + 1$, is chosen in a way that $\Delta x = \Delta x = 0.01$. Then, the solution to the problem can be approximated by considering the system

$$C_T \frac{u_{i,j+1} - u_{i,j}}{\Delta t} = \frac{u_{i-1,j+1}\kappa_{i-\frac{1}{2}} - u_{i,j+1}\left(\kappa_{i-\frac{1}{2}} + \kappa_{i+\frac{1}{2}}\right) + u_{i+1,j+1}\kappa_{i+\frac{1}{2}}}{\Delta x^2}$$

$$+ R(x_i, u_{i,j+1}) + \sqrt{\frac{\Delta t}{\Delta x}}\sigma z_{i,j} \quad 0 \le i \le n, 0 \le j \le m-1,$$

$$0 = \frac{u_{n+1,j} - u_{n-1,j}}{2\Delta x} = \frac{u_{1,j} - u_{-1,j}}{2\Delta x} \quad j = 1, \ldots, m,$$

$$u_{i,0} = u_W(x_i), \quad i = 0, \ldots, n,$$

where $u_{-1,j}, u_{n+1,j}$ are ghost points, $(z_{i,j})_{i,j}$ is a collection of independent identically distributed (i.i.d.) normal random variables, and $u_{i,j} = u(x_i, t_j)$, $\kappa_{i\pm\frac{1}{2}} = \kappa\left(x_{i\pm\frac{1}{2}}\right)$, $x_{i\pm\frac{1}{2}} = x_i \pm \Delta x/2$. Since $u_{1,j} = u_{-1,j}$ and $u_{n+1,j} = u_{n-1,j}$, the previous system of equation can be rewritten as

$$(I_{n+1} - rA)\,\underline{u}^{j+1} = I_{n+1}\underline{u}^j + \frac{\Delta T}{C_T}\underline{R}(\underline{u}^{j+1}) + \sqrt{\frac{\Delta t}{\Delta x}}\sigma\underline{Z}^j,$$

where I_{n+1} denotes the $(n+1) \times (n+1)$ identity matrix, $\underline{u}^j = \left(u_{0,j}, \ldots, u_{n,j}\right)^T$, $r = \frac{\Delta t}{C_T \Delta x^2}$, $\underline{R}(\underline{y}) = \left(R(x_0, y_1), \ldots, R(x_n, y_{n+1})\right)^T$, $\left(\underline{Z}^j\right)_j$ denotes a set of i.i.d. $\mathcal{N}(\underline{0}, I_{n+1})$ normal random vectors, and

$A \in \mathbb{R}^{(n+1)\times(n+1)}$ is the tridiagonal matrix with diagonal $\underline{d} \in \mathbb{R}^{n+1}$, superdiagonal $\underline{d}_1 \in \mathbb{R}^n$, and subdiagonal $\underline{d}_{-1} \in \mathbb{R}^n$ given by

$$\underline{d}(i) = \begin{cases} -(\kappa_{-1/2} + \kappa_{1/2}), & i = 1, \\ -(\kappa_{i-3/2} + \kappa_{i-1/2}), & i = 2, \ldots, n, \\ -(\kappa_{n-1/2} + \kappa_{n+1/2}), & i = n+1, \end{cases}$$

$$\underline{d}_1(i) = \begin{cases} \kappa_{-1/2} + \kappa_{1/2}, & i = 1, \\ \kappa_{i-1/2}, & i = 2, \ldots, n, \end{cases}$$

$$\underline{d}_{-1}(i) = \begin{cases} \kappa_{i-1/2} + \kappa_{1/2}, & i = 1, \ldots, n, \\ -(\kappa_{n-1/2} + \kappa_{n+1/2}), & i = n. \end{cases}$$

Thus, given the numerical approximation $\underline{u}^j$ at time t_j, to advance the scheme at time t_{j+1} it is needed to solve the previous non-linear system of algebraic equations. To do this, we apply the Newton–Raphson Method (NRM), which we recall in the following. We consider the map $\underline{F}^j \colon \mathbb{R}^{n+1} \to \mathbb{R}^{n+1}$ defined as

$$\underline{F}^j(\underline{y}) = (I_{n+1} - rA)\,\underline{y} - \underline{u}^j - \frac{\Delta T}{C_T}\underline{R}(\underline{y}) - \sqrt{\frac{\Delta t}{\Delta x}}\sigma\underline{Z}^j.$$

To approximate the vector $\underline{y} \in \mathbb{R}^{n+1}$ such that $\underline{F}^j(\underline{y}) = 0$, the NRM consider the following sequence

$$\begin{cases} \underline{y}^{k+1} = \underline{y}^k - J_{F^j}(\underline{y}^k)^{-1}F^j(\underline{y}^k), \\ \underline{y}^0 = \underline{u}^j, \end{cases}$$

where $J_{\underline{F}^j} \in \mathbb{R}^{(n+1)\times(n+1)}$ is the Jacobian matrix of $\underline{F}^j$ with respect to $\underline{y}$. Since the noise intensity $\sigma = 0.2$ is small, we expect that the choice $\underline{y}^0 = \underline{u}_j$ is a good initial guess of the solution. The iteration of the NRM is stopped when $\|\underline{F}^j(\underline{y}^k)\| \leq 10^{-10}$.

APPENDIX B: SPECTRAL PROPERTIES OF THE OPERATOR $\tilde{A}$

To apply the invariant measure theory, the operator $\tilde{A} = \lambda Id - A$ defined in Sec. III D should satisfy the following assumptions (see Ref. 48, Sec. 11):

(i) $\tilde{A}$ is self-adjoint and there exists $\omega > 0$ such that

$$\langle \tilde{A}x, x \rangle \leq -\omega|x|^2, \quad x \in D(A).$$

(ii) There exists $\beta \in (0,1)$ such that $Tr\left[(-\tilde{A})^{\beta-1}\right] < +\infty$.

We denote by $(\lambda_n)_n$ the eigenvalues of $-A$, where

$$\begin{aligned} D(A) &= \left\{ u \in H^2(-1,1) \mid u'(-1) = u'(1) = 0 \right\}, \\ Au &= \left(\kappa(x)u'\right)'. \end{aligned} \tag{B1}$$

Since A is a Sturm–Liouville regular operator, classical results assure the existence of the real eigenvalues λ_n, and furthermore, it can be proved

$$\lambda_1 < \lambda_2 < \cdots\cdots < \lambda_n < \cdots \to +\infty.$$

First, to check hypothesis (i), it is thus sufficient to prove that

$$\lambda_n \geq 0, \quad \forall n.$$

Indeed, by definition of eigenvalue, there exists an eigenfunction $v_n \in D(A)$ such that

$$Av_n = -\lambda_n v_n.$$

Multiplying the previous identity by v_n and integrating over the domain $[-1,1]$, we get

$$\int_{-1}^{1}\left[\kappa(x)v'_n(x)\right]' v_n(x)\,dx = -\lambda_n\int_{-1}^{1}v_n(x)^2\,dx.$$

Performing an integration by parts on the left-hand side, we deduce

$$-\int_{-1}^{1}\kappa(x)\left(v'_n(x)\right)^2\,dx = -\lambda_n\int_{-1}^{1}v_n(x)^2\,dx.$$

In conclusion,

$$\lambda_n = \frac{\int_{-1}^{1}\kappa(x)\left(v'_n(x)\right)^2\,dx}{\int_{-1}^{1}v_n(x)^2\,dx},$$

and our claim follows from the fact that $\kappa(x) > 0$ on $[-1,1]$.

Second, the hypothesis (ii) is a consequence of the following asymptotic estimate for regular Sturm–Liouville problems (Ref. 52, Sec. 4): there exist $B > 0$ and $n_0 > 0$ such that

$$\left[\frac{\left(n - \frac{1}{2}\right)\pi}{B}\right]^2 < \lambda_n < \left[\frac{\left(n + \frac{1}{2}\right)\pi}{B}\right]^2, \quad \forall n \geq n_0.$$

REFERENCES

[1] *Climate Change 2001: The Scientific Basis*, Contribution of Working Group I to the Third Assessment Report of the Intergovernmental Panel on Climate Change, edited by J. T. Houghton, Y. Ding, D. J. Griggs, M. Noguer, P. J. van der Linden, X. Dai, K. Maskell, and C. A. Johnson (Cambridge University Press, 2001).

[2] V. Dakos, M. Scheffer, E. H. van Nes, V. Brovkin, V. Petoukhov, and H. Held, "Slowing down as an early warning signal for abrupt climate change," Proc. Natl. Acad. Sci. **105**, 14308–14312 (2008).

[3] M. Scheffer, J. Bascompte, W. Brock, V. Brovkin, S. Carpenter, V. Dakos, H. Held, E. Nes, M. Rietkerk, and G. Sugihara, "Early-warning signals for critical transitions," Nature **461**, 53–9 (2009).

[4] C. Kuehn, "A mathematical framework for critical transitions: Bifurcations, fast–slow systems and stochastic dynamics," Physica D **240**, 1020–1035 (2011).

[5] P. Ashwin, S. Wieczorek, R. Vitolo, and P. Cox, "Tipping points in open systems: Bifurcation, noise-induced and rate-dependent examples in the climate system," Philos. Trans. R. Soc. A **370**, 1166–1184 (2012).

[6] T. M. Lenton, V. N. Livina, E. H. van Nes, and M. Scheffer, "Early warning of climate tipping points from critical slowing down: Comparing methods to improve robustness," Philos. Trans. R. Soc. A **370**, 1185–1204 (2012).

[7] M. Ghil and V. Lucarini, "The physics of climate variability and climate change," Rev. Mod. Phys. **92**, 035002 (2020).

[8] P. Bernuzzi and C. Kuehn, "Bifurcations and early-warning signs for spdes with spatial heterogeneity," J. Dyn. Differ. Equ. (published online, 2023).

[9] M. Dewey and C. Goldblatt, "Evidence for radiative-convective bistability in tropical atmospheres," Geophys. Res. Lett. **45**, 10673–10681, https://doi.org/10.1029/2018GL078903 (2018).

[10] M. I. Budyko, "The effect of solar radiation variations on the climate of the earth," Tellus A **21**, 611–619 (2022).

[11] W. D. Sellers, "A global climatic model based on the energy balance of the earth-atmosphere system," J. Appl. Meteorol. Climatol. **8**, 392–400 (1969).

[12] G. R. North, "Theory of energy-balance climate models," J. Atmos. Sci. **32**, 2033–2043 (1975).

[13] M. Ghil, "Climate stability for a sellers-type model," J. Atmos. Sci. **33**, 3–20 (1976).

[14] J. I. Díaz, "On the mathematical treatment of energy balance climate models," in *The Mathematics of Models for Climatology and Environment*, edited by J. I. Díaz (Springer, Berlin, 1997), pp. 217–251.

[15] P. Cannarsa, V. Lucarini, P. Martinez, C. Urbani, and J. Vancostenoble, "Analysis of a two-layer energy balance model: Long time behavior and greenhouse effect," Chaos **33**, 113111 (2023).

[16] G. R. North and K.-Y. Kim, *Energy Balance Climate Models* (Wiley, 2017).

[17] K. Emanuel, A. A. Wing, and E. M. Vincent, "Radiative-convective instability," J. Adv. Model. Earth Syst. **6**, 75–90 (2014).

[18] T. Beucler and T. W. Cronin, "Moisture-radiative cooling instability," J. Adv. Model. Earth Syst. **8**, 1620–1640 (2016).

[19] G. Da Prato and J. Zabczyk, *Ergodicity for Infinite Dimensional Systems*, London Mathematical Society Lecture Note Series (Cambridge University Press, 1996).

[20] G. Da Prato and J. Zabczyk, *Stochastic Equations in Infinite Dimensions* (Cambridge University Press, 2014).

[21] K. Hasselmann, "Stochastic climate models part I. Theory," Tellus **28**, 473–485 (1976).

[22] M. I. Freidlin and A. D. Wentzell, *Random Perturbations of Dynamical Systems* (Springer, Berlin, 2012).

[23] L. Arnold, "Hasselmann's program revisited: The analysis of stochasticity in deterministic climate models," in *Stochastic Climate Models*, edited by P. Imkeller and J.-S. von Storch (Birkhäuser, Basel, 2001), pp. 141–157.

[24] Y. Kifer, "Averaging and climate models," in *Stochastic Climate Models* (Springer, 2001), pp. 171–188.

[25] F. Flandoli, U. Pappalettera, and E. Tonello, "Nonautonomous attractors and young measures," Stochastics Dyn. **22**, 2240003 (2022).

[26] H. Crauel and F. Flandoli, "Attractors for random dynamical systems," Probab. Theory Relat. Fields **100**, 365–393 (1994).

[27] L. Arnold, *Random Dynamical Systems*, Springer Monographs in Mathematics (Springer-Verlag, Berlin, 1998), p. xvi+586.

[28] M. Ghil, M. D. Chekroun, and E. Simonnet, "Climate dynamics and fluid mechanics: Natural variability and related uncertainties," Physica D **237**, 2111–2126 (2008).

[29] M. D. Chekroun, E. Simonnet, and M. Ghil, "Stochastic climate dynamics: Random attractors and time-dependent invariant measures," Physica D **240**, 1685–1700 (2011).

[30] D. Dommenget and J. Flöter, "Conceptual understanding of climate change with a globally resolved energy balance model," Clim. Dyn. **37**, 2143–2165 (2011).

[31] R. Bastiaansen, H. A. Dijkstra, and A. S. von der Heydt, "Fragmented tipping in a spatially heterogeneous world," Environ. Res. Lett. **17**, 045006 (2022).

[32] G. Del Sarto, J. Bröcker, F. Flandoli, and T. Kuna, "Variational techniques for a one-dimensional energy balance model," Nonlinear Processes Geophys. **31**, 137–150 (2024).

[33] C. E. Graves, W.-H. Lee, and G. R. North, "New parameterizations and sensitivities for simple climate models," J. Geophys. Res.: Atmos. **98**, 5025–5036 (1993).

[34] P. Baldi, *Stochastic Calculus* (Springer International Publishing, 2017).

[35] R. Temam, *Infinite-Dimensional Dynamical Systems in Mechanics and Physics* (Springer, New York, 1997).

[36] J. Smoller, *Shock Waves and Reaction—Diffusion Equations* (Springer Science & Business Media, 2012), Vol. 258.

[37] G. Floridia, "Approximate controllability for nonlinear degenerate parabolic problems with bilinear control," J. Differ. Equ. **257**, 3382–3422 (2014).

[38] P. Cannarsa, M. Malfitana, and P. Martinez, "Parameter determination for energy balance models with memory," in *Mathematical Approach to Climate Change and Its Impacts: MAC2I* (Springer International Publishing, 2020), pp. 83–130.

[39] G. Myhre, A. Myhre, and F. Stordal, "Historical evolution of radiative forcing of climate," Atmos. Environ. **35**, 2361–2373 (2001).

[40] I. P. on Climate Change (IPCC), *Climate Change 2021—The Physical Science Basis: Working Group I Contribution to the Sixth Assessment Report of the Intergovernmental Panel on Climate Change* (Cambridge University Press, 2023).

[41] G. Myhre, E. J. Highwood, K. P. Shine, and F. Stordal, "New estimates of radiative forcing due to well mixed greenhouse gases," Geophys. Res. Lett. **25**, 2715–2718, https://doi.org/10.1029/98gl01908 (1998).

[42] G. R. North, L. Howard, D. Pollard, and B. Wielicki, "Variational formulation of Budyko-Sellers climate models," J. Atmos. Sci. **36**, 255–259 (1979).

[43] G. R. North, "Multiple solutions in energy balance climate models," Global Planet. Change **2**, 225–235 (1990).

[44] H. Brezis, *Functional Analysis, Sobolev Spaces and Partial Differential Equations* (Springer, 2011), Vol. 2.

[45] P. Imkeller, "Energy balance models—Viewed from stochastic dynamics," in *Stochastic Climate Models*, edited by P. Imkeller and J.-S. von Storch (Birkhäuser, Basel, 2001), pp. 213–240.

[46] J. Díaz, J. Langa, and J. Valero, "On the asymptotic behaviour of solutions of a stochastic energy balance climate model," Physica D **238**, 880–887 (2009).

[47] G. Díaz and J. I. Díaz, "Stochastic energy balance climate models with legendre weighted diffusion and an additive cylindrical wiener process forcing," Discrete Contin. Dyn. Syst. **15**, 2837–2870 (2022).

[48] G. Da Prato, *An Introduction to Infinite-Dimensional Analysis* (Springer, Berlin, 2006).

[49] D. B. Stephenson, H. Diaz, and R. Murnane, "Definition, diagnosis, and origin of extreme weather and climate events," Clim. Extremes Soc. **340**, 11–23 (2008).

[50] L. Lombroso and S. Quattrocchi, *L'osservatorio di Modena: 180 Anni di Misure Meteoclimatiche* (SMS, 2008).

[51] G. J. Lord, C. E. Powell, and T. Shardlow, *An Introduction to Computational Stochastic PDEs*, Cambridge Texts in Applied Mathematics (Cambridge University Press, 2014).

[52] C. Fulton and S. Pruess, "Eigenvalue and eigenfunction asymptotics for regular Sturm-Liouville problems," J. Math. Anal. Appl. **188**, 297–340 (1994).

[53] G. Del Sarto (2024). "A non-autonomous framework for climate change and extreme weather events increase in a stochastic energy balance model – Numerical code," Zenodo. https://doi.org/10.5281/zenodo.11609953